

Effects of density- and momentum-dependent potentials in Au+Au collisions at intermediate energies^{*}

Wen-Jie Xie(谢文杰)^{1,1)} Feng-Shou Zhang(张丰收)²

¹ Department of Physical and Electronic Engineering, Yuncheng University, Yuncheng 044000, China

² The Key Laboratory of Beam Technology and Material Modification of Ministry of Education, College of Nuclear Science and Technology, Beijing Normal University, Beijing 100875, China

Abstract: Based on an isospin-dependent transport model, the effects of the density- and momentum-dependent potentials are studied by simulating Au on Au collisions at 90, 120, 150 and 400 MeV/nucleon. It is found that the calculated results overestimate the experimental data on the directed flow and underestimate the data on the elliptic flow for protons. The impact of the density- and momentum-dependent potentials is observed in the mid-rapidity region of the final spectra. At 90 MeV/nucleon, the momentum-dependent potential has a larger impact on the observables than the density-dependent potential, and the elliptic flow has a higher value with the positive effective mass splitting. At 400 MeV/nucleon, however, the opposite is observed. The rapidity dependence of the elliptic flow for protons is sensitive to the symmetry energy. A soft symmetry energy corresponds to a higher value of the proton elliptic flow.

Keywords: symmetry energy, effective mass splitting, nuclear collective flow, Au+Au collisions

PACS: 25.75.Dw, 21.65.-f, 21.30.Fe **DOI:** 10.1088/1674-1137/42/10/104103

1 Introduction

The isospin-dependence of the nuclear equation of state (EOS), generally known as symmetry energy, $E_{\text{sym}}(\rho)$, is the most important but poorly known property of neutron-rich matter [1]. Constraints on the symmetry energy in neutron-rich matter have been an interesting subject of study over the past two decades. Numerous theoretical studies [2–12] and experimental measurements [11–17] have been devoted to the study of the nuclear symmetry energy at both subsaturation and suprasaturation densities; for recent reviews, see Ref. [18]. So far the symmetry energy at subsaturation densities has been relatively well constrained by comparing the theoretical results with the experimental data on isospin diffusion and the ratios of neutron and proton multiplicities in heavy ion collisions [4, 6]. However, the case at suprasaturation densities still remains uncertain.

According to the contribution of the symmetry energy, we have

$$E_{\text{sym}}(\rho) = E_{\text{sym}}^{\text{kin}}(\rho) + E_{\text{sym}}^{\text{loc}}(\rho) + E_{\text{sym}}^{\text{mom}}(\rho). \quad (1)$$

The first term in Eq. (1) is the kinetic energy and can

be written as

$$E_{\text{sym}}^{\text{kin}}(\rho) = \frac{1}{3} \frac{\hbar^2}{2m} \left(\frac{3}{2} \pi^2 \rho \right)^{2/3}. \quad (2)$$

The second and third terms in Eq. (1) are the local and the momentum-dependent parts, respectively. The local part corresponds to the density-dependent symmetry potential and the momentum-dependent part corresponds to the momentum-dependent symmetry potential. Therefore, to constrain the symmetry energy, knowledge of the density- and the momentum-dependent symmetry potentials is required. In non-relativistic transport models, the momentum-dependent potential leads to the neutron-proton effective mass splitting $m_n^* - m_p^*$, where m_n^* and m_p^* represent the neutron and proton effective masses, respectively. Positive ($m_n^* > m_p^*$) and negative ($m_n^* < m_p^*$) effective mass splittings correspond to completely different momentum-dependent symmetry potentials [19–22]. Unfortunately, the constraint on the neutron-proton effective mass splitting is highly controversial [23].

One of the forms for the momentum-dependent symmetry potential stems from the Gale-Bertsch-Das-Gupta (GBD) force, which has been widely used in the Boltzmann-Uehling-Uhlenbeck models [24–26]. It

Received 4 May 2018, Published online 24 August 2018

^{*} Supported by National Natural Science Foundation of China (11505150), China Postdoctoral Science Foundation (2015M582730) and Yuncheng University Research Project (YQ-2014014)

1) E-mail: wenjiexie@yeah.net

©2018 Chinese Physical Society and the Institute of High Energy Physics of the Chinese Academy of Sciences and the Institute of Modern Physics of the Chinese Academy of Sciences and IOP Publishing Ltd

is found that the sensitivity to the symmetry energy is suppressed as compared to that for the momentum-dependent symmetry potential [26]. The momentum-dependent symmetry potential plays an important role in understanding the mechanisms of fast nucleon emission [27] and nuclear collective flow [19]. Based on the real Skyrme potential energy density, Zhang et al. improved the quantum molecular dynamics model (ImQMD05) by including the energy density of isospin-dependent Skyrme-like momentum-dependent interactions [28]. Based on the momentum-dependent potential derived from the measured energy dependence of the proton-nucleus optical potential [29], Feng et al. incorporated a Skyrme-like momentum-dependent symmetry potential into the QMD model [20, 30], which is used in the present work.

In this article, based on the isospin-dependent quantum molecular dynamics model developed at Beijing Normal University (IQMD-BNU) [21, 22, 31–36], the effects of the density- and momentum-dependent symmetry potentials are investigated via calculating the collective flow of protons produced in the reaction Au+Au in the incident energy range from 90 to 400 MeV/nucleon. The article is organized as follows. In Section 2, we give a description of the recent version of the IQMD-BNU model. The calculated results for the proton collective flows are shown and discussed in Section 3. In Section 4, conclusions are given.

2 Theoretical approach

In QMD-like models, the time evolution of nucleons in the system are governed by the Hamiltonian equations of motion, which read

$$\dot{\mathbf{p}}_i = -\frac{\partial H}{\partial \mathbf{r}_i}, \quad \dot{\mathbf{r}}_i = \frac{\partial H}{\partial \mathbf{p}_i} \quad (3)$$

with \mathbf{r}_i and \mathbf{p}_i standing for the average values of the position and momentum for the i th nucleon. The Hamiltonian H of nucleons and resonances in the present QMD version is constructed by

$$H = \sum_i \sqrt{p_i^2 + m_i^2} + U_{\text{coul}} + U_{\text{mdi}} + \int V_{\text{loc}}[\rho(\mathbf{r})]d\mathbf{r}, \quad (4)$$

where the first term on the right-hand side of Eq. (4) is the kinetic energy. The second term is the Coulomb potential energy and is written as

$$U_{\text{coul}} = \frac{1}{2} \sum_{i,j,i \neq j} \frac{e_i e_j}{r_{ij}} \text{erf}\left(\frac{r_{ij}}{\sqrt{4L}}\right) \quad (5)$$

with e_i representing the electric charge of nucleons or resonances, and $r_{ij} = |\mathbf{r}_i - \mathbf{r}_j|$ the relative distance between two charged particles. The third term in Eq. (4) denotes the momentum-dependent potential energy.

Generally, the nucleon energy density consists of two parts, namely the local and non-local parts. The local potential density used in the present work reads

$$V_{\text{loc}}(\rho) = \frac{\alpha}{2} \frac{\rho^2}{\rho_0} + \frac{\beta}{\gamma+1} \frac{\rho^{\gamma+1}}{\rho_0^\gamma} + \frac{g_{\text{sur}}}{2} \frac{(\nabla\rho)^2}{\rho_0} + E_{\text{sym}}^{\text{loc}}(\rho)\rho\delta^2, \quad (6)$$

with

$$E_{\text{sym}}^{\text{loc}}(\rho) = \frac{1}{2} C_{\text{sym}} \left(\frac{\rho}{\rho_0}\right)^{\gamma_s}. \quad (7)$$

Here α , β , γ , g_{sur} and ρ_0 are taken as -390 MeV, 320 MeV, 1.14 , 130 MeV \cdot fm 5 and 0.16 fm $^{-3}$, respectively, and the corresponding compressibility is 200 MeV. $\delta = (\rho_n - \rho_p)/\rho$ is the isospin asymmetry, where ρ_n and ρ_p stand for the neutron and proton densities, respectively. Equation (7) gives the soft and hard cases of the symmetry energy with $\gamma_s = 0.5$ and 2.0 . The non-local potential density reads [37]

$$U_{\text{mdi}} = \frac{1}{2\rho_0} \sum_{\tau,\tau',\tau \neq \tau'} C_{\tau,\tau'} \int \int \int d\mathbf{p}d\mathbf{p}'d\mathbf{r} \times f_\tau(\mathbf{r},\mathbf{p}) \ln^2[t_5(\mathbf{p}-\mathbf{p}')^2+1] f_{\tau'}(\mathbf{r},\mathbf{p}'). \quad (8)$$

The coefficient t_5 in Eq. (8) has the value of 0.0005 MeV $^{-2}$, $C_{\tau,\tau} = t_4(1-x)$ and $C_{\tau,\tau'} = t_4(1+x)$ with $t_4 = 1.57$ MeV. The parameters x and C_{sym} are taken to be -0.65 and 52.5 MeV respectively for the positive mass splittings, and 0.65 and 23.52 MeV respectively for the negative mass splittings [37]. The slope parameter L , which is calculated by $L = 3\rho_0(\partial E_{\text{sym}}/\partial\rho)|_{\rho=\rho_0}$, is 201.5 MeV for the hard symmetry energy and 83.6 MeV for the soft symmetry energy. According to Eqs. (6), (7) and (8), one can obtain the single-particle potential used in the QMD-BNU model as:

$$U_\tau(\rho, \delta, \mathbf{p}) = \alpha \frac{\rho}{\rho_0} + \beta \left(\frac{\rho}{\rho_0}\right)^\gamma + U_\tau^{\text{sym}} + U_\tau^{\text{mom}}, \quad (9)$$

with

$$U_\tau^{\text{sym}} = E_{\text{sym}}^{\text{loc}}(\rho)\delta^2 + \frac{\partial E_{\text{sym}}^{\text{loc}}(\rho)}{\partial\rho}\rho\delta^2 + E_{\text{sym}}^{\text{loc}}(\rho)\rho\frac{\partial\delta^2}{\partial\rho_\tau}, \quad (10)$$

and

$$U_\tau^{\text{mom}} = \frac{C_{\tau,\tau}}{\rho_0} \int d\mathbf{p}' f_\tau(\mathbf{r},\mathbf{p}) \ln^2[t_5(\mathbf{p}-\mathbf{p}')^2+1] + \frac{C_{\tau,\tau'}}{\rho_0} \int d\mathbf{p}' f_{\tau'}(\mathbf{r},\mathbf{p}) \ln^2[t_5(\mathbf{p}-\mathbf{p}')^2+1], \quad (11)$$

where U_τ^{sym} denotes the part which corresponds to the density-dependent symmetry energy and U_τ^{mom} is the momentum-dependent part.

Shown in Figs. 1 and 2 are U_τ^{sym} (shown by solid lines), and U_τ^{mom} (shown by dashed lines) as a function of momentum for two cases of the symmetry energy and the nucleon effective mass splitting with isospin asymmetry $\delta=0.2$ at $\rho = \rho_0$ and $\rho = 2\rho_0$, respectively, where ρ_0 represents the saturation density. One can

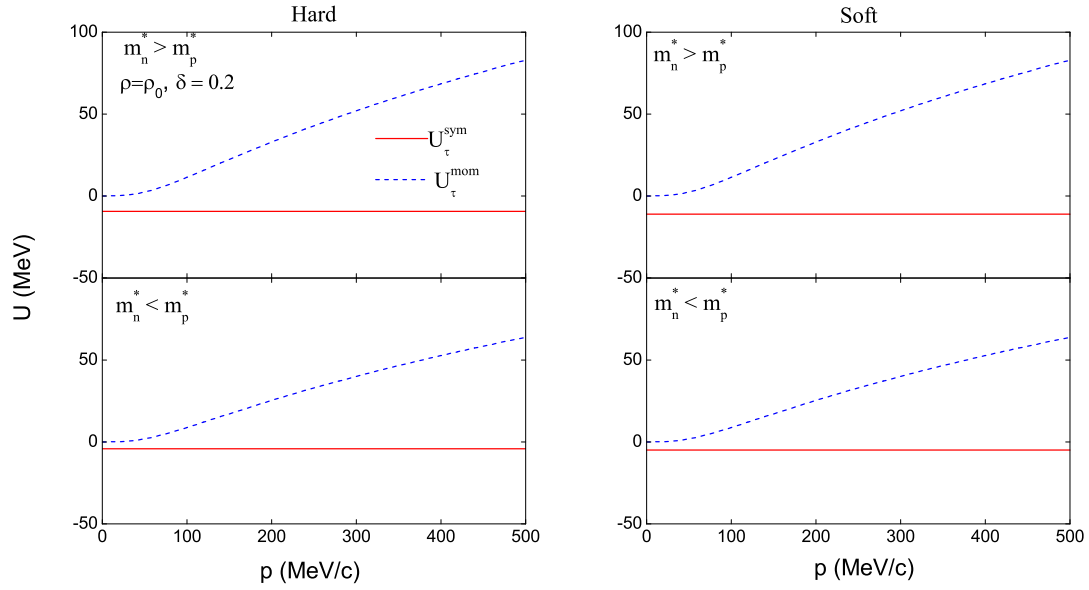


Fig. 1. (color online) Single-particle potentials that correspond to the density-dependent symmetry energy (solid lines), and to the momentum-dependent interactions (dashed lines) for protons as a function of momentum for two sets of the symmetry energy and the nucleon mass splitting at $\rho=\rho_0$ with isospin asymmetry $\delta=0.2$.

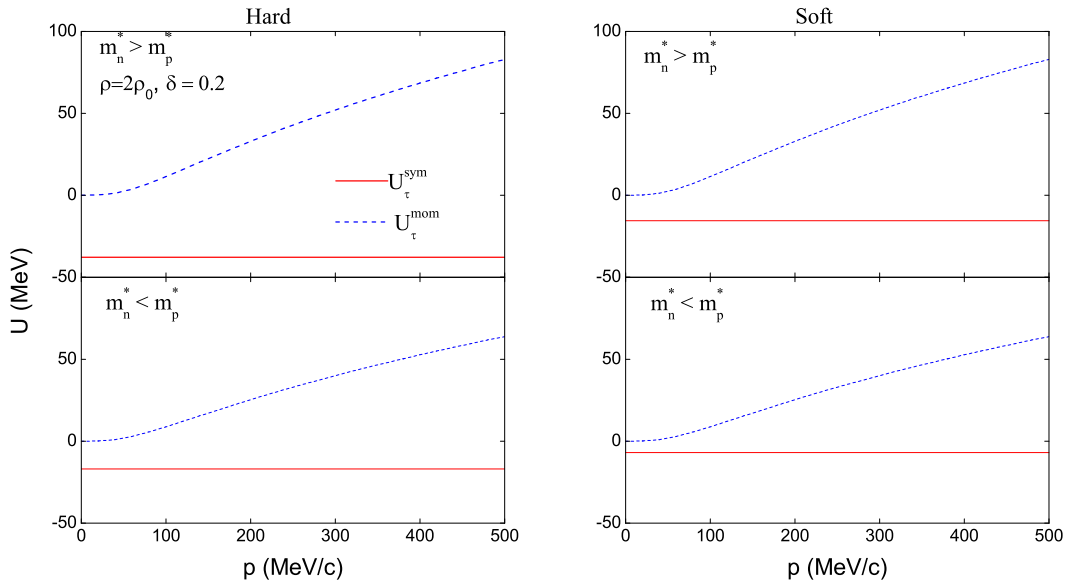


Fig. 2. (color online) Single-particle potentials that correspond to the density-dependent symmetry energy (solid lines), and to the momentum-dependent interactions (dashed lines) for protons as a function of momentum for two sets of the symmetry energy and the nucleon mass splitting at $\rho=2\rho_0$ with isospin asymmetry $\delta=0.2$.

see that protons suffer a repulsive (attractive) force due to the momentum-dependent (density-dependent) potential. With increasing momentum, the momentum-dependent potential has different values in comparison with the density-dependent one. Moreover, this difference changes when the nucleon density, the nucleon effective mass splitting, and the symmetry energy are different. Protons suffer more repulsion when we take the positive mass splitting, as shown in Fig. 3.

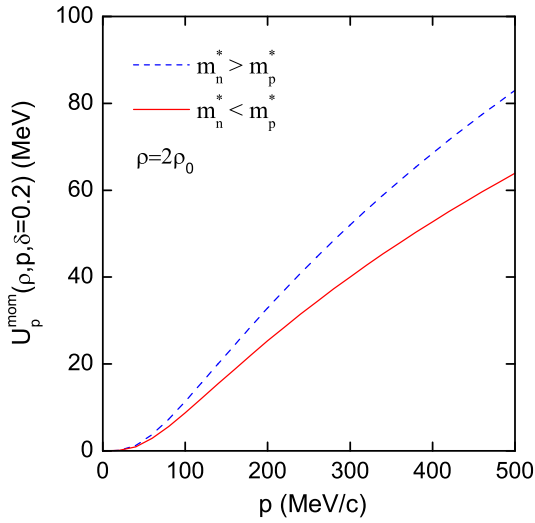


Fig. 3. (color online) Momentum-dependent potential for protons as a function of momentum for two sets of the nucleon mass splitting with $\delta=0.2$ at $\rho=2\rho_0$.

The method to deal with two-nucleon collisions is same as in the cascade model [39]. The cross sections in free space, from Ref. [40], are taken for the elastic channels and the cross sections in the medium are taken for the inelastic channels. The in-medium modification factor for the inelastic channels has the form of $1-0.2\rho/\rho_0$ [41]. Pauli blocking and the constraint on the phase space density used in the constrained molecular dynamics (CoMD) approach [42] are included in the model to take the fermionic nature of the nucleon into consideration.

3 Results and discussion

In Figs. 4, 5 and 6 we plot the rapidity dependence of the directed flow, $v_1(y_0)$, the transverse momentum dependence of the directed flow, $v_1(u_{t0})$, and the transverse momentum dependence of the elliptic flow, $v_2(u_{t0})$, for protons produced in Au+Au collisions at 90, 120 and 150 MeV/nucleon respectively, with centrality $0.25 < b_0 < 0.45$ and various cuts as indicated in the figures. Here

y_0 , u_{t0} and b_0 are same as in Ref. [16]. The directed and elliptic flows are respectively defined by

$$v_1 = \left\langle \frac{p_x}{p_t} \right\rangle = \langle \cos(\phi) \rangle, \quad (12)$$

and

$$v_2 = \left\langle \frac{(p_x^2 - p_y^2)}{p_t^2} \right\rangle = \langle \cos(2\phi) \rangle. \quad (13)$$

The quantities p_x and p_y represent the momentum components, and $p_t = \sqrt{p_x^2 + p_y^2}$ denotes the transverse momentum of a nucleon. The angular brackets stand for the average over all events, and ϕ is the azimuth with respect to the reaction plane. The free protons are obtained by using a coalescence model, in which nucleons with relative momentum $p_0 \leq 300$ MeV and relative distance $r_0 \leq 3.0$ fm are coalesced into a cluster [38].

In the calculations two cases of the symmetry energy and the effective mass splitting are taken, as indicated in the figures. It is found that the rapidity dependence of the directed flow for protons is sensitive to both the symmetry energy and the effective mass splitting in Au+Au collisions at 90 MeV/nucleon. The values obtained from the hard symmetry energy (the positive effective mass splitting) are larger than those from the soft symmetry energy (the negative effective mass splitting). This can be explained by the fact that more protons get unbound due to the hard symmetry energy (the positive effective mass splitting) with respect to the soft symmetry energy (the negative effective mass splitting) at subsaturation densities. However, this sensitivity becomes weaker as the incident energy increases. This is because, with increasing incident energy, the pressure coming from the isospin-dependent mean-field potential (symmetry potential part) is weaker than that from the isospin-independent and kinetic parts [22, 43]. The total effect caused by the effective mass splitting and the density-dependent symmetry energy is quite weak. For the transverse momentum distributions of the directed flow and the elliptic flow, one cannot extract information on the symmetry energy and the effective mass splitting. Our calculated results slightly overestimate the experimental data taken by the FOPI collaboration [17]. It is difficult to interpret the difference between the calculated results and the data. As stated in Ref. [44], one of the main reasons for the overestimation is the in-medium modification factor for the nucleon-nucleon cross section. The theoretical values will approach the experimental results if we take a stronger modification factor.

Shown in Fig. 7 is the rapidity dependence of the elliptic flow for protons in Au+Au collisions at 150 MeV/nucleon with the transverse velocity cut $u_{t0} > 0.8$ and centrality $0.25 < b_0 < 0.45$. In the mid-rapidity region, the v_2 values calculated by using the positive effective mass splitting are larger than those obtained from the negative case. This can be understood by the fact

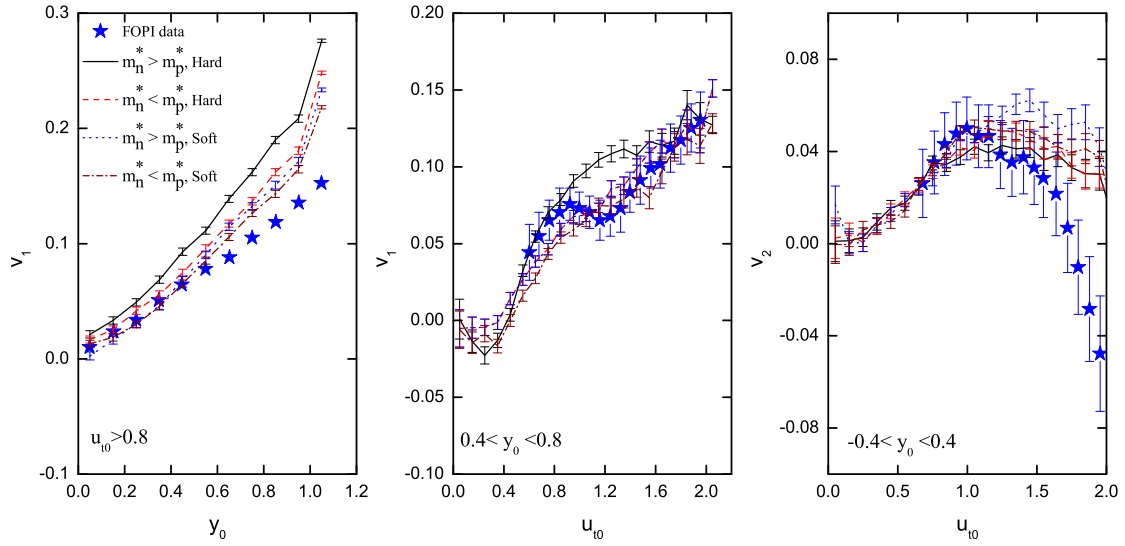


Fig. 4. (color online) Left panel: Rapidity dependence of the directed flow with the transverse velocity cut $u_{t0} > 0.8$. Middle panel: Transverse momentum dependence of the directed flow with the longitudinal rapidity cut $0.4 < y_0 < 0.8$. Right panel: Transverse momentum dependence of the elliptic flow with the longitudinal rapidity cut $-0.4 < y_0 < 0.4$. The results are calculated for protons produced in the reaction Au+Au at 90 MeV/nucleon with centrality $0.25 < b_0 < 0.45$. The experimental data are taken from Ref. [17].

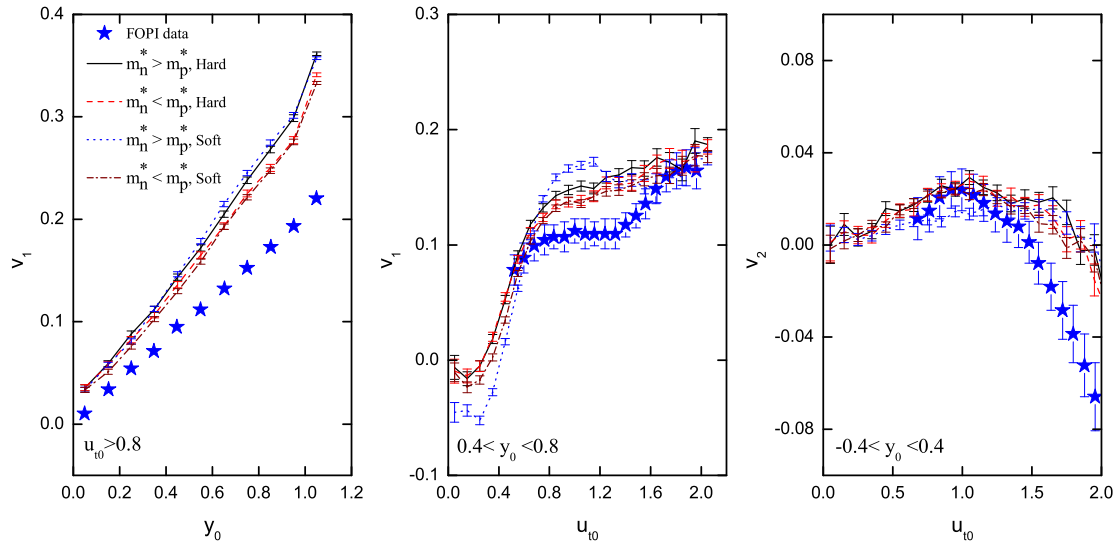


Fig. 5. (color online) Left panel: Rapidity dependence of the directed flow with the transverse velocity cut $u_{t0} > 0.8$. Middle panel: Transverse momentum dependence of the directed flow with the longitudinal rapidity cut $0.4 < y_0 < 0.8$. Right panel: Transverse momentum dependence of the elliptic flow with the longitudinal rapidity cut $-0.4 < y_0 < 0.4$. The results are calculated for protons produced in the reaction Au+Au at 120 MeV/nucleon with centrality $0.25 < b_0 < 0.45$. The experimental data are taken from Ref. [17].

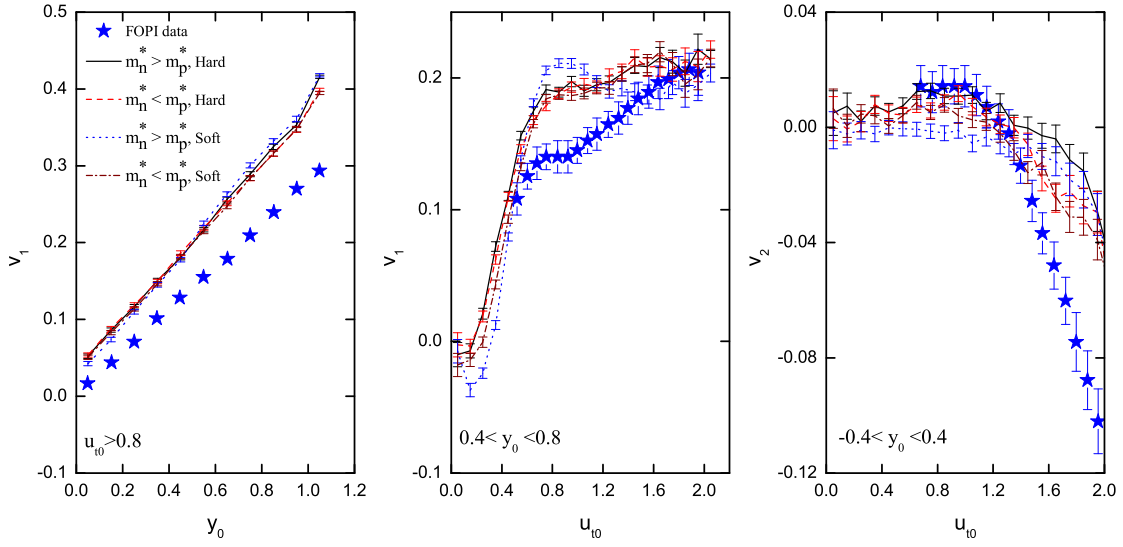


Fig. 6. (color online) Left panel: Rapidity dependence of the directed flow with the transverse velocity cut $u_{t0} > 0.8$. Middle panel: Transverse momentum dependence of the directed flow with the longitudinal rapidity cut $0.4 < y_0 < 0.8$. Right panel: Transverse momentum dependence of the elliptic flow with the longitudinal rapidity cut $-0.4 < y_0 < 0.4$. The results are calculated for protons produced in the reaction Au+Au at 150 MeV/nucleon with centrality $0.25 < b_0 < 0.45$. The experimental data are taken from Ref. [17].

that protons calculated with the positive effective mass splitting suffer more repulsive force than those with the negative effective mass splitting.

In Fig. 8, we show the rapidity dependence of the elliptic flow for protons in Au+Au collisions at 400 MeV/nucleon with the transverse velocity cut $u_{t0} > 0.4$ and centrality $0.25 < b_0 < 0.45$. For the impact of the effective mass splitting, as shown in the left-hand panel of Fig. 8, it is found that, contrary to the results in the mid-rapidity region of Fig. 7, the v_2 values obtained with negative mass splitting are larger than those calculated with the positive mass splitting. This is because, in the mid-rapidity region, the system is in a high-density state and the density-dependent symmetry potential is stronger than the momentum-dependent one, as shown in Fig. 2. The effects of the neutron-proton effective mass splitting are cancelled by the effect of the density-dependent potential. For the impact of the symmetry energy, as shown in the right-hand panel of Fig. 8, we can see that the proton elliptic flow has a larger value for the soft symmetry energy than for the hard symmetry energy. The high-density region is more proton-rich with a higher symmetry energy and consequently more free protons are squeezed out with a lower symmetry energy. Moreover, this phenomenon becomes more pronounced as the transverse velocity cut increases, as indicated in Fig. 9. Our calculated results can describe the experimental data relatively well.

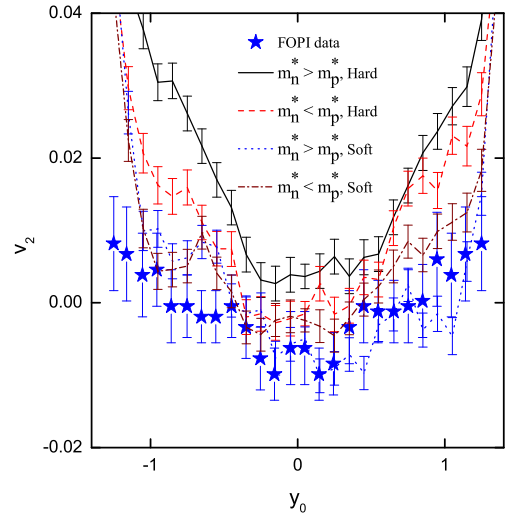


Fig. 7. (color online) Rapidity dependence of the elliptic flow for protons in the reaction Au+Au at 150 MeV/nucleon with the transverse velocity cut $u_{t0} > 0.8$ and centrality $0.25 < b_0 < 0.45$. Various cases of the symmetry energy and the effective mass splitting are used in the calculations as indicated. The experimental data are taken from Ref. [17].

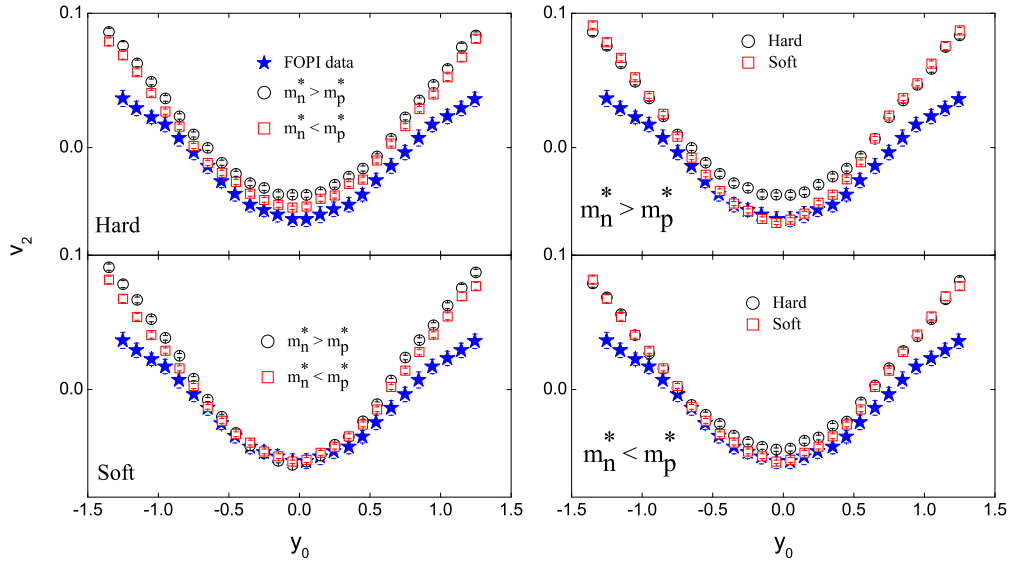


Fig. 8. (color online) Rapidity distributions of the elliptic flow for protons in the reaction Au+Au at 400 MeV/nucleon with the transverse velocity cut $u_{t0} > 0.4$ and centrality $0.25 < b_0 < 0.45$. Two cases of the symmetry energy and the effective mass splitting are used in the calculations as indicated. The experimental data are taken from Ref. [17].

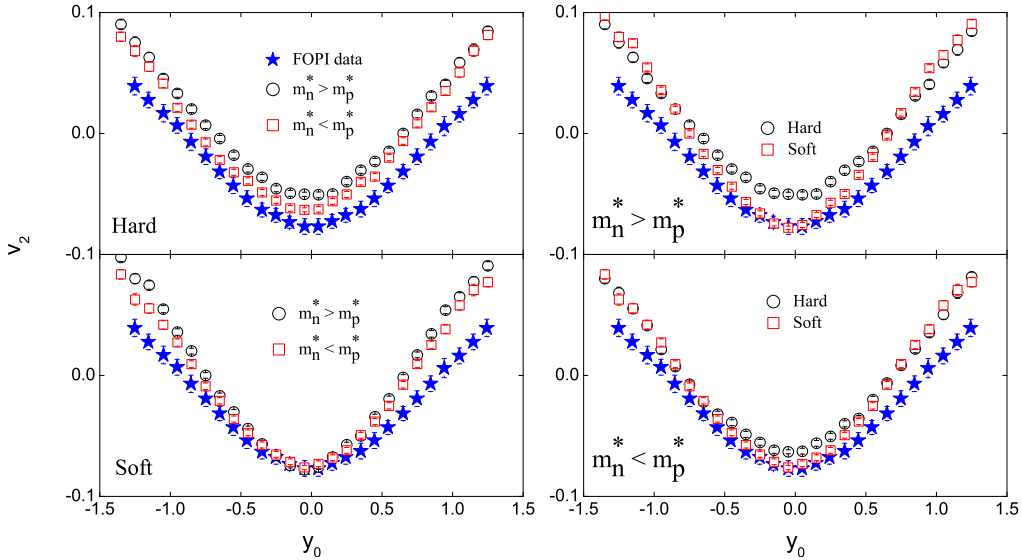


Fig. 9. (color online) Rapidity distributions of the elliptic flow for protons in the reaction Au+Au at 400 MeV/nucleon with the transverse velocity cut $u_{t0} > 0.8$ and centrality $0.25 < b_0 < 0.45$. Two cases of the symmetry energy and the effective mass splitting are used in the calculations as indicated. The experimental data are taken from Ref. [17].

4 Conclusions

In summary, we have investigated the effects of the density- and momentum-dependent potentials via calculating the directed and elliptic flows for protons produced in Au on Au collisions at 90, 120, 150 and 400 MeV/nucleon with centrality of $0.25 < b_0 < 0.45$ in the framework of the IQMD-BNU model. It is found that the directed flow is sensitive to both the neutron-proton effective mass splitting and the symmetry energy at 90 MeV/nucleon, but this sensitivity disappears as the incident energy increases. Our results for the rapidity distributions of the directed flow, and the transverse momentum distributions of the directed flow and elliptic

flow, overestimate the experimental data. At lower incident energies, such as 90 MeV/nucleon, the momentum-dependent potential plays a more important role than the density-dependent potential, and the elliptic flow has a higher (lower) value with the positive (negative) effective mass splitting. However, at 400 MeV/nucleon, the opposite phenomenon is observed, with the elliptic flow having a higher (lower) value with the negative (positive) effective mass splitting. This is different from the results in Ref. [19]. The elliptic flow has a higher (lower) value with a soft (hard) symmetry energy.

We thank Prof. Zhao-Qing Feng for fruitful discussions.

References

- 1 Isospin Physics in Heavy-Ion Collisions at Intermediate Energies, edited by B. A. Li and W. Udo Schröder (Nova Science, New York, 2001)
- 2 B. A. Li, L. W. Chen, C. M. Ko, Phys. Rep., **464**: 113 (2008)
- 3 V. Baran, M. Colonna, V. Greco, and M. Di Toro, Phys. Rep., **410**: 335 (2005)
- 4 M. B. Tsang, Y. Zhang, P. Danielewicz, M. Famiano, Z. Li, W. G. Lynch, A. W. Steiner, Phys. Rev. Lett., **102**: 122701 (2009)
- 5 G. Ferini, T. Gaitanos, M. Colonna, M. Di Toro, H. H. Wolter, Phys. Rev. Lett., **97**: 202301 (2006)
- 6 L. W. Chen, C. M. Ko, B. A. Li, Phys. Rev. Lett., **94**: 032701 (2005)
- 7 J. B. Natowitz, G. Röpke, S. Typel, D. Blaschke, A. Bonasera, K. Hagel, T. Klähn, S. Kowalski, L. Qin, S. Shlomo, R. Wada, H. H. Wolter, Phys. Rev. Lett., **104**: 202501 (2010)
- 8 Z. G. Xiao, B. A. Li, L. W. Chen, G. C. Yong, and M. Zhang, Phys. Rev. Lett., **102**: 062502 (2009)
- 9 Z. Q. Feng, G. M. Jin, Phys. Lett. B, **683**: 140 (2010)
- 10 W. J. Xie, J. Su, L. Zhu, and F. S. Zhang, Phys. Lett. B., **718**: 1510 (2013)
- 11 P. Russotto, P. Z. Wu, M. Zoric, M. Chartier, Y. Leifels, R. C. Lemmon, Q. Li, J. Lukasik, A. Pagano, P. Pawłowski, and W. Trautmann, Phys. Lett. B, **697**: 471 (2011)
- 12 F. Amorini, et al, Phys. Rev. Lett., **102**: 112701 (2009)
- 13 T. X. Liu et al, Phys. Rev. C, **86**: 024605 (2012)
- 14 Z. Kohley et al, Phys. Rev. C, **82**: 064601 (2010)
- 15 M. B. Tsang et al, Phys. Rev. Lett., **92**: 062701 (2004)
- 16 W. Reisdorf et al, Nucl. Phys. A, **781**: 459 (2007)
- 17 W. Reisdorf et al, Nucl. Phys. A, **876**: 1 (2012)
- 18 Topical issue on nuclear symmetry energy, edited by B. A. Li, A. Ramos, G. Verde and I. Vidaña (Eur. Phys. J. A, volume 50, 2014)
- 19 V. Giordano, M. Colonna, M. Di Toro, V. Greco, and J. Rizzo, Phys. Rev. C, **81**: 044611 (2010)
- 20 Z. Q. Feng, Phys. Lett. B, **707**: 83 (2012)
- 21 W. J. Xie, J. Su, L. Zhu, F. S. Zhang, Phys. Rev. C, **88**: 061601(R) (2013)
- 22 W. J. Xie and F. S. Zhang, Phys. Lett. B, **735**: 250 (2014)
- 23 B. A. Li, B. J. Cai, L. W. Chen, and J. Xu, Prog. Part. Nucl. Phys., **99**: 29 (2018)
- 24 C. Gale, G. M. Welke, M. Prakash, S. J. Lee, and S. Das Gupta, Phys. Rev. C, **41**: 1545 (1990)
- 25 C. B. Das, S. D. Gupta, C. Gale, and B. A. Li, Phys. Rev. C., **67**: 034611 (2003)
- 26 B. A. Li, C. B. Das, S. D. Gupta, C. Gale, Phys. Rev. C, **69**: 011603(R) (2004)
- 27 J. Rizzo, M. Colonna, and M. Di Toro, Phys. Rev. C, **72**: 064609 (2005)
- 28 Y. Zhang, M. B. Tsang, Z. Li, H. Liu, Phys. Lett. B, **732**: 186 (2014)
- 29 J. Aichelin, A. Rosenhauer, G. Peilert, H. Stoecker, and W. Greiner, Phys. Rev. Lett., **58**: 1926 (1987)
- 30 Z. Q. Feng, Phys. Rev. C, **84**: 024610 (2011)
- 31 L. W. Chen, F. S. Zhang, and G. M. Jin, Phys. Rev. C, **58**: 2283 (1998)
- 32 J. Su, K. Cherevko, W. J. Xie, and F. S. Zhang, Phys. Rev. C, **89**: 014619 (2014)
- 33 B. A. Bian, F. S. Zhang, and H. Y. Zhou, Phys. Lett. B, **665**: 314 (2008)
- 34 L. Zhu, J. Su, W. J. Xie, and F. S. Zhang, Nucl. Phys. A, **915**: 90 (2013)
- 35 J. Su and F. S. Zhang, Phys. Rev. C, **84**: 037601 (2011)
- 36 J. Su, L. Zhu, W. J. Xie, and F. S. Zhang, Phys. Rev. C, **85**: 017604 (2012)
- 37 Z. Q. Feng, Phys. Rev. C, **85**: 014604 (2012)
- 38 W. J. Xie, Z. Q. Feng, J. Su, F. S. Zhang, Phys. Rev. C, **91**: 054609 (2015)
- 39 G. F. Bertsch and S. Das Gupta, Phys. Rep., **160**: 189 (1988)
- 40 J. Cugnon, D. L'Hôte, and J. Vandermeulen, Nucl. Instrum. Meth. Phys. Res. B, **111**: 215 (1996)
- 41 G. D. Westfall, et al, Phys. Rev. Lett., **71**: 1986 (1993)
- 42 M. Papa, T. Maruyama, and A. Bonasera, Phys. Rev. C, **64**: 024612 (2001)
- 43 B. A. Li, A. T. Sustich, B. Zhang, Phys. Rev. C, **64**: 054604 (2001)
- 44 Y. Wang, C. Guo, Q. Li, H. Zhang, Z. Li, and W. Trautmann, Phys. Rev. C, **89**: 034606 (2014); Q. Li, C. Shen, C. Guo, Y. Wang, Z. Li, J. Lukasik, and W. Trautmann, Phys. Rev. C, **83**: 044617 (2011)